



UNIVERSITÀ POLITECNICA DELLE MARCHE
Repository ISTITUZIONALE

Comparing Mobile Laser Scanner and manual measurements for dendrometric variables estimation in a black pine (*Pinus nigra* Arn.) plantation

This is the peer reviewed version of the following article:

Original

Comparing Mobile Laser Scanner and manual measurements for dendrometric variables estimation in a black pine (*Pinus nigra* Arn.) plantation / Chiappini, S; Pierdicca, R; Malandra, F; Tonelli, E; Malinverni, Es; Urbinati, C; Vitali, A. - In: COMPUTERS AND ELECTRONICS IN AGRICULTURE. - ISSN 0168-1699. - 198:(2022). [10.1016/j.compag.2022.107069]

Availability:

This version is available at: 11566/306080 since: 2024-03-26T14:34:12Z

Publisher:

Published

DOI:10.1016/j.compag.2022.107069

Terms of use:

The terms and conditions for the reuse of this version of the manuscript are specified in the publishing policy. The use of copyrighted works requires the consent of the rights' holder (author or publisher). Works made available under a Creative Commons license or a Publisher's custom-made license can be used according to the terms and conditions contained therein. See editor's website for further information and terms and conditions.

This item was downloaded from IRIS Università Politecnica delle Marche (<https://iris.univpm.it>). When citing, please refer to the published version.

(Article begins on next page)

23 Comparing Mobile Laser Scanner and manual
24 measurements for dendrometric variables estimation in
25 a black pine (*Pinus nigra* Arn.) plantation

26 Stefano Chiappini^a, Roberto Pierdicca^b, Francesco Malandra^a, Enrico
27 Tonelli^a, Eva Savina Malinverni^a, Carlo Urbinati^a, Alessandro Vitali^b

^a*Department of Agricultural, Food and Environmental Sciences, Marche Polytechnic University, Ancona, 60100, Italy, alessandro.vitali@univpm.it (A.V.); f.malandra@univpm.it (F.M.); e.tonelli@pm.univpm.it (E.T.); c.urbinati@univpm.it (C.U.)*

^b*Department of Civil Engineering, Construction and Architecture, Marche Polytechnic University, Ancona, 60100, Italy, r.pierdicca@univpm.it (R.P.); s.chiappini@pm.univpm.it (S.C.); e.s.malinverni@univpm.it (E.M.)*

28 **Abstract**

The growing demand of ecosystem services provided by forests increased the need for fast and accurate field survey. The recent technological innovations fostered the application of geomatic tools and processes to different fields of the forestry sector. In this study we compared the efficiency and the accuracy of Mobile Laser Scanner (MLS), combined with Simultaneous Localization and Mapping (SLAM) technology, and traditional field survey for the mensuration of main forest dendrometric variables like stem diameter at breast height (DBH), individual tree height (H), crown base height (CBH) and **branch-free** stem volume (VOL). With ground truth measurements taken from 50 felled trees, we tested the applicability of MLS technology for individual tree parameters estimation in a conifer plantation in central Italy. Our results showed no bias of DBH estimates and the corresponding RMSE was equal to 10.8% (2.7 cm). H and CBH measured with MLS were underes-

estimated compared to the ground truth (bias of -8.6% for H and -13.3% for CBH). VOL values showed a bias and a RMSE of -4.1% (-0.01 m^3) and 12.4% (0.04 m^3) respectively. Tree height is not perfectly estimated due to laser obstruction by crowns layer, but the acquisition speed of this survey, joined with a suitable accuracy of parameters extraction, suggests sufficient suitability of the method for operational applications in simple forest structures (e.g. one-layered stands).

29 *Keywords:* **LiDAR** Mobile laser scanning, forest inventory, tree detection,
30 conifer plantation

31 **1. Introduction**

32 The accurate measurement of forest stand features is not only a scientific value *per se* but a fundamental step in silvicultural management and
33 forest planning. There is an increasing need for accurate and fast forest field
34 inventories, due also to the growing demand for the assessment of the multiple ecosystem services (Müller et al., 2020). Besides the widespread use,
35 in the last decades, of remote sensing techniques in forest inventories, the
36 operational surveys still require manual measurements of field plots (Hyypä
37 et al., 2020a). Diameter at breast height (DBH), individual tree height (H)
38 and crown base height (CBH) are the tree parameters most frequently measured in the field. Although traditional field measurements are as yet broadly
39 practised, they present some bottlenecks being time consuming and limited
40 in their spatial extent (Bauwens et al., 2016).
41
42
43

44 *1.1. Geomatic meets forestry: 3D data acquisition and processing.*

45 Current forestry management practices, can benefit from different survey-
46 ing approaches: Terrestrial Laser Scanning (TLS), Airborne Laser Scanning
47 (ALS), Mobile Laser Scanning (MLS) and Personal Laser Scanning (PLS, a
48 subcategory of MLS). DBH, H, CBH and other tree variables can be esti-
49 mated using either the ALS system (Luo et al., 2018; Maguya et al., 2015;
50 Sibona et al., 2017), the TLS survey (de Conto et al., 2017; Liu et al., 2018a)
51 or the MLS technology (Čerňava et al., 2017; Forsman et al., 2016). In this
52 scenario, the increasing consciousness and the availability of technological in-
53 novations have made possible a stronger bond between geomatic and forestry
54 disciplines. Forest inventory at different scales and levels of detail plays a key
55 role for the management choices and the geomatic techniques can increase the
56 automation level during the field measurements (Pierzchała et al., 2018). In-
57 deed, over the last decades, technological development in data collection and
58 computational processes have opened up new fields of research, also in for-
59 est data analysis, using remote and proximal sensing approaches (Tao et al.,
60 2015). Then, the forestry point cloud data analysis and management can be
61 conducted using different softwares, as argued by several studies in the lit-
62 erature: CloudCompare (Girardeau-Montaut, 2021), FUSION/LDT (Karna
63 et al., 2019; Moe et al., 2020), LiDAR 360 (Chen et al., 2019; Luo et al., 2018),
64 "3D Forest" (Trochta et al., 2017), Computree (Del Perugia et al., 2019),
65 MATLAB (Itakura and Hosoi, 2020; Zhang et al., 2019), Python (Holmgren
66 et al., 2019; Srinivasan et al., 2015), R packages such as "lidR" (Tompalski
67 et al., 2019; Zaforemska et al., 2019), "TreeLS" (Dalla Corte et al., 2020;
68 Puliti et al., 2020) and "rLiDAR" (Mohan et al., 2017).

69 *1.2. The need for ground-based mobile proximal sensing.*

70 The rapid development of acquisition systems able to collect 3D point
71 clouds, allowed the automation of forest inventory procedures. Several plat-
72 forms have been developed to reduce time and cost of traditional measure-
73 ments held with optical or electronic instruments and to improve their pre-
74 cision and accuracy (Luoma et al., 2017; Wang et al., 2019). Light detec-
75 tion and ranging (LiDAR) techniques is boosting ecological and forest re-
76 search, and researchers in various fields began to apply it for modelling anal-
77 ysis (Zhou et al., 2019). TLS is a ground based LiDAR scanning system
78 able to offer data to analyze, improving significantly Above-Ground Biomass
79 (AGB) estimation (Stovall et al., 2017). The 3D model derived by TLS
80 application are treated as ground truth validation of forest biomass models
81 (Momo Takoudjou et al., 2018; Brede et al., 2019). From these data is pos-
82 sible to extract and storing different metric data, such as DBH (Liu et al.,
83 2018b; Dassot et al., 2012), H (Panagiotidis et al., 2016; Cabo et al., 2018),
84 stem volume (Iizuka et al., 2020; Panagiotidis and Abdollahnejad, 2021a,b),
85 AGB (Momo Takoudjou et al., 2018; Gonzalez de Tanago et al., 2018) and
86 branch architecture (Lau et al., 2018). Unfortunately, due to the static nature
87 of TLS, it requires multiple scanning stations to ensure the effective detec-
88 tion of the trees. This task is time-consuming and requires manpower (Kunz
89 et al., 2019). The most significant problems are the effects of the occlusion by
90 trunks, crown and the understory vegetation (Bauwens et al., 2016; Gollob
91 et al., 2020; Holopainen et al., 2013a). The limitation listed on TLS have
92 boosted researchers to move up technologies able to produce 3D point clouds
93 in a ready to use manner.

94 A solution is given by mobile laser scanner (MLS) (Mokroš et al., 2021).
95 These systems combine a laser scanner with an inertial measurement unit
96 (IMU), exploiting the so called SLAM (Simultaneous Localization and Map-
97 ping). The accuracy of measurements mainly depends by the synchronization
98 of these components. Moreover, thanks to the moving platform, the occlusion
99 effect is reduced (Bauwens et al., 2016). MLS applications are divided in two
100 categories: handheld laser scanning (HMLS) and backpack personal laser
101 scanning (BMLS). Early scientific publications with MLS date back 2013,
102 and the first system prototype was large in size and weighed approximately
103 30 kg, which limited its operability and mobility (Kukko et al., 2012). More
104 recent *out-of-the-shelves* products are lighter and more compact than more
105 complex MLS systems, and can be easily held by a single operator even in
106 challenging scenario. Several studies evaluate the accuracy of these different
107 scanning systems in forestry settings. Comparative studies between TLS and
108 MLS revealed that MLS got more accuracy than TLS rate (Gollob et al.,
109 2020), and took less time to collect the data. The use of TLS requires mul-
110 tiple scanning bases to ensure the effective detection of the trees, and the
111 most significant problems are the effects of shade or concealment by trees
112 (Bauwens et al., 2016; Gollob et al., 2019). Conversely, some studies on the
113 quality of the point cloud obtained by MLS report a problem in the model
114 due to noise (Bauwens et al., 2016) or errors in fitting the geometric shapes
115 (Nurunnabi et al., 2017). In order to achieve high accuracy, several factors
116 must be taken into account, such as a small research plot, the best envi-
117 ronmental conditions, the instrument used and visibility of the surrounding
118 environment during real-time mapping (Van Brummelen et al., 2018).

119 1.3. Paper contribution

120 Given the above-mentioned aspects and in line with the recent litera-
121 ture, in this study we tested the applicability of MLS technology to measure
122 individual tree parameters in a black pine (*Pinus nigra* Arn.) plantation.
123 Specifically, we first compared three methodologies of MLS point cloud pro-
124 cessing to obtain DBH, H, CBH and **branch-free stem** VOL on standing trees
125 and estimated their accuracy. Then, we compared the best MLS-derived and
126 traditional manual-measured values with the ground truth data collected
127 from selected felled trees. From the experiments, we hypothesized that DBH
128 estimation could be affected by less error than total height and crown base
129 height, due to the limitation of crown shielding.

130 2. Materials and methods

131 2.1. Study Area

132 The study area is included in the “Cesane Regional Forest” (43°42’N
133 12°45’E), a large forest area of approximately 1500 ha located on the homony-
134 mous mountain system in the norther part of the Marche region in Central
135 Italy. The orographic system is ranging from 200 to 600 m a.s.l. featuring
136 smooth hills and some steep slopes, with an extended top plateau. The forest
137 became state owned a century ago to be restored with reafforestation after
138 intensive agro-pastoral exploitation causing extended slope erosion. Forest
139 plantation, often along man-made stone terraces, started in the early ‘900 but
140 continued especially after World War II using mainly a very resilient conifer
141 species such as *Pinus nigra* var. *nigra*, well adapted even to bare rocky soils.
142 Pine is by far the dominant species (Figure 1) with a mean stand density

143 equal to 800 n/ha, but manna ash (*Fraxinus ornus* L.) was also frequently
144 planted along the rows. In addition we found a very sporadic occurrence of
145 downy oak (*Quercus pubescens* Willd., 1805), sycamore maple (*Acer pseudo-*
146 *platanus* L., 1753) and European smoke tree (*Cotinus coggygria* Scop.) that
147 have probably entered naturally in the forest area.

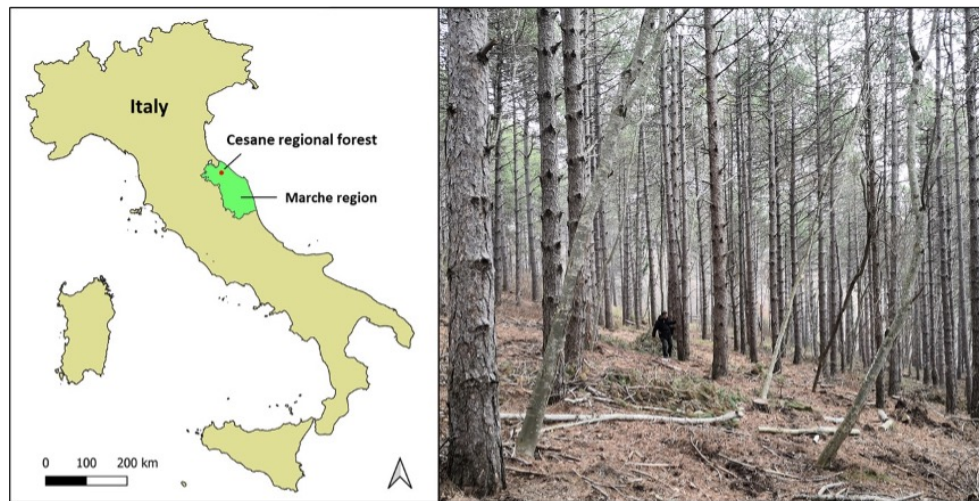


Figure 1: The location of the study area (left) and a view of the black pine plantation (right)

148 2.2. MLS survey

149 The survey was conducted in early February 2020 to reduce the occlusion
150 effect caused by deciduous species of the understory, with a Mobile Mapping
151 System device Kaarta Stencil 2¹. This instrumentation is equipped with a
152 LiDAR Velodyne VLP-16 sensor mounted on top of an aluminum platform,
153 an IMU (Internal MEMS) and an internal processor (Intel-7) for real-time

¹<https://www.kaarta.com/products/stencil-2-for-rapid-long-range-mobile-mapping>

154 localization and mapping. This instrument scans the environment around the
 155 device, quickly and automatically, in 'handheld' mode. It is a light weight
 156 (1730 grams) device, with battery life of around 2 hours and internal 1 Tb
 157 SSD memory. It provides a very dense point detection (300000 maximum
 158 number of points to read from the logged up to 10 Hz). The LiDAR has
 159 a beam ($\lambda = 903$ nm) with 16 laser profiles and a vertical field of view
 160 of $+15^\circ$ to -15° , while the horizontal view is 360° . The scanning path was
 161 performed considering the following issues: i) avoiding occlusions among
 162 trees, maximizing the best coverage for the trees; ii) reducing the drift error,
 163 which may occur in repetitive environments where the alignment is harder;
 164 iii) avoiding the noise in the point cloud data. For the above-mentioned
 165 reasons, we adopted the following settings (Table 1).

Table 1: Kaarta Stencil 2 parameters setting used for field survey.

Parameters	Value [m]
VoxelSize	0.4
registrationRadius	100
cornerVoxelSize	0.2
surfVoxelSize	0.4
surroundVoxelSize	0.6
blindRadius	1.0

166 The scan survey covered approximately 0.5 ha of the forest stand and
 167 it was conducted walking through the forest plantation rows. The study
 168 area was surveyed in 75 minutes collecting 276 millions of points with a reg-
 169 istration radius value of 100 meters (Figure 2a). During the MLS survey,

170 it also has been possible to view the operations carried out by the tracker
171 camera on an external monitor. Concluded these steps, the system created
172 and currently dated a folder with files describing the configuration settings,
173 3D cloud characteristics and trajectory estimation. Since the Kaarta is not
174 equipped with an internal GNSS, it has been necessary to manually per-
175 form the georeferencing post-process of the point cloud using CloudCompare
176 tools (Kruček et al., 2020). We then collected the coordinates (x,y) of three
177 Ground Control Points (GCPs) with a HiPer VR Topcon GNSS antenna² in
178 the centre of three reflective targets placed on the ground at a considerable
179 distance, projected in the WGS 84-UTM33N coordinate reference system.

180 *2.3. Traditional field survey and ground truth assessment with felled trees*

181 Within the MLS scanned area, we selected 50 pines of representative tree
182 diameter and height within the pine stand (Figure 2b). We first traditionally
183 measured the 50 standing trees: DBH with a dendrometric caliper, H and
184 CBH (the height from the tree stem base up to the first living tree branch)
185 with a Haglöf Hypsometer (Vertext III). We also registered the relative tree
186 positions measuring with sub-metric precision their horizontal distance and
187 azimuth with a TruPulse 360B rangefinder (Laser Technology Inc.) from five
188 GCP recorded with the HiPer VR Topcon GNSS receiver. The DBH of the
189 selected trees ranged from 13.5 to 37.0 cm, with a mean and median value
190 of 24.9 cm and 25.3 cm respectively.

191 In a second step, the selected 50 trees were cut down in September 2020
192 after authorization from the regional authority. We measured the stems total

²<https://www.topconpositioning.com/it/support/products/hiper-vr>

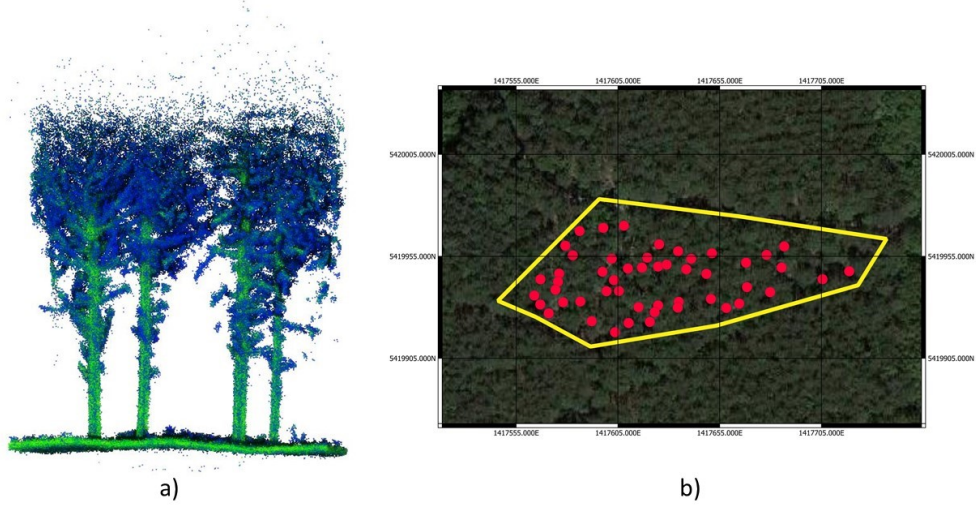


Figure 2: a) an example of the tree point cloud view by Kaarta Stencil 2; b) distribution of the 50 selected trees (red dots) within the yellow boundary of the forest plot .

193 length (equal to the tree height) of felled trees with a measuring tape and the
 194 length from the stem base to the first living branch (corresponding to CBH).
 195 Stem diameter was measured at the stem base, at 1.30 m (corresponding to
 196 DBH) and at the median line of every 1 m long virtual sections from the
 197 base to the tapering diameter of 7 cm. The **branch-free stem** height was
 198 determined by visual interpretation of the stem profile, until a mean cut off
 199 height of 8 m. The **branch-free** volume (VOL) of single felled stems was
 200 computed applying the Heyer's formula (equation 1):

$$V = S_1 + S_2 + S_3 + \dots S_{n-1} + S_n \quad (1)$$

201 where V is the volume up to 8 meters above the ground and S_1, S_2, S_{n-1}
 202 are the transversal surface areas of each 1 m long log. We assumed that

203 collected measures on felled trees were error free and we used them as refer-
204 ence data for the comparison with traditional measurements and with remote
205 sensed records.

206 *2.4. Point cloud processing*

207 For better comprehension we outlined the data processing workflow in
208 Figure 3.

209 We analyzed the points cloud by developing a semi-automatic approach
210 for the extraction of metric data. The first phase concerns importing and
211 visualising the raw data in CloudCompare (Girardeau-Montaut, 2021); then,
212 we filtered the raw cloud by removing unnecessary detected areas to make
213 its management easier. After having delimited the test area, we performed
214 data filtering using the "Statistical outlier remover" SOR function (Rusu and
215 Cousins, 2011) which allows to discard outliers and noise points produced on
216 the trunks surface during the acquisition phase. Then, we carried out the
217 classification between the ground and above ground points, using the Cloth
218 Simulation Filter (CSF). CSF filters the terrain points, ensuring significant
219 time savings and accurate reliability of the final data. The values adopted
220 to set the parameters, optimized after several tests, were 0.3 m cloth resolu-
221 tion and 0.6 m distance threshold, with a maximum of 50 iterations for the
222 analysed sample. Since some portions of the trunk were classified as ground
223 points (Figure 4) it required further filtering using the "Features Geometric"
224 tool which classifies all point verticality concerning the nearest neighbours
225 point, based on the local orientation and curvature of the stem point cloud
226 (Hackel et al., 2016). For this project, "TreeLS" package (de Conto et al.,
227 2017) was used to segment the whole point cloud forest and to get a point

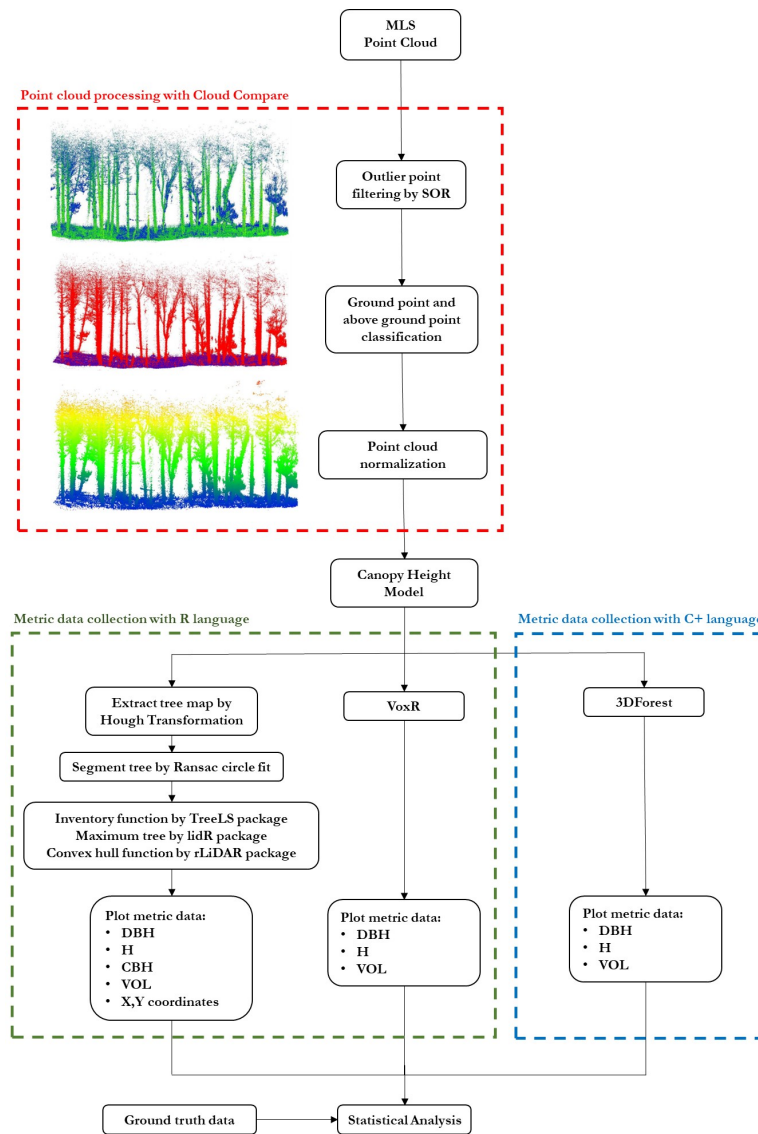


Figure 3: Research Workflow (Diameter at breast height (DBH), individual tree height (H), crown base height (CBH), branch-free stem volume(VOL), barycentric coordinates (X,Y)).

228 cloud for each individual tree, which calculates the vertical area and enables
 229 visual detection of surfaces that extend perpendicularly to the ground. Af-

230 ter normalizing the points cloud, we automatically extracted a set of metric
231 data belonging to each of the 50 felled pines for statistical evaluation. We
232 manually matched the coordinates of the extracted trees with those collected
233 in the field with the laser rangefinder , both data were registered in the same
234 reference system (WGS84-UTM33N).

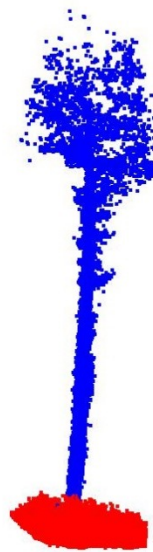


Figure 4: The individual output from Cloth Simulated Filter (CFS) algorithm. The ground points are red and off-ground points blue.

235 For this scope, we analysed several data extraction methodologies. More
236 in deep, for the detection of forest metrics we exploited the "3D Forest" open
237 source application (Trochta et al., 2017), "VoxR" package and the combina-
238 tion of "TreeLS-rLiDAR-lidr" packages inside R language (R Core Team,
239 2021). Afterward, we compared these methods with ground truth data.
240 The first method is "3D Forest" application, based on the C++ language
241 and widely used to analyze points clouds from Terrestrial Laser Scanning.

242 This is based on clustering points according to their relative distance, mini-
243 mum number, corner and distance between centroids of each cluster (Kruček
244 et al., 2020). This application is suitable for processing trees with simple
245 crown structure, reason why it has severely limited the extraction of further
246 data. In fact, the irregular crown shape and dense foliage limited a correct
247 investigation, such as the segmentation and volume of branches, leading to
248 discordant results. Therefore in this case we calculated DBH, H and **branch-**
249 **free stem** VOL (Figure 5a). The tool allows the extraction of two different
250 DBH, the first Randomized Hough transformation (RHT) according to the
251 circle detected in the point analysis, whereas the second one, based on Least
252 Square Regression, with an algebraic estimate of the geometry calculation of
253 the detected circle (Chernov and Lesort, 2005). Next, we defined H as the
254 calculation of the maximum distance between the two points along the Z axis.
255 Finally, we computed the **branch-free stem** volume using the Convex hull al-
256 gorithm. At the end of this procedure, a denoising operation was used to
257 filter out those points not belonging to the trees. Noise reduction and clean-
258 ing operations are included in CloudCompare. The second test consisted on
259 running the "VoxR" package (Lecigne et al., 2018), a library written with the
260 R language (Team et al., 2013) which is based on a voxelization algorithm
261 that has allowed the classification of points in a regular three-dimensional
262 grid of voxels (Fernández-Sarría et al., 2013). The file, imported in .txt for-
263 mat, was subjected to metric analysis, using the "tree_metrics" function and
264 setting the voxel size as 0.05 m; DBH, H and VOL values were extracted
265 (cylinder), such as diameter, height, and volume (Figure 5b). This func-
266 tion makes the metric data extraction easy and intuitive. The third method

267 tested is a set of R-packages allowing the extraction of the whole metric data.
268 TreeLS (de Conto et al., 2017) permits the users to customize the parameters
269 according to the tree characteristics and the points clouds, using algorithms
270 with various functions. The most important one allows the stem mapping
271 through the automatic detection of individual trunk points. We carried out
272 the correct identification of the trunk’s points, separating it from the branches
273 and leaves by means of the Hough transformation and consequently exploit-
274 ing the RANSAC algorithm (de Conto et al., 2017). The latter subdivides
275 the cloud into several subsets, providing the inventory of each calculated ge-
276 ometric primitive (cylinder), such as diameter, height, and volume (Figure
277 5c). The last step generates a series of geometric primitives of cylindrical
278 shape along the vertical axis of the trunk. Before being reconstructed by
279 using the geometrical primitive, in particular the circular cylinders (Markku
280 et al., 2015), the stem point cloud tree was sliced in to three subclasses. This
281 necessary because of stem tapering as also addressed by Panagiotidis and
282 Abdollahnejad (2021b). The slicing step has carried out along the z-axis
283 from up to the maximum height of 8 metres for each investigated tree. We
284 calculated a cylinder primitive geometrical by Ransac algorithm. It was
285 filtered on vertical point cloud slice with high accuracy. Thus, the output a
286 high details and accuracy concerning the metric data, such as DBH, H and
287 **branch-free stem** volume.

288 This choice derived from LiDAR data that provide an incomplete repre-
289 sentation of the trunk surface, due to physical obstacles (fallen trees, shrubs
290 or saplings) or shaded areas. In particular, denoising operations tend to
291 poorly filter out even heterogeneous or unshaded portions of point clouds,

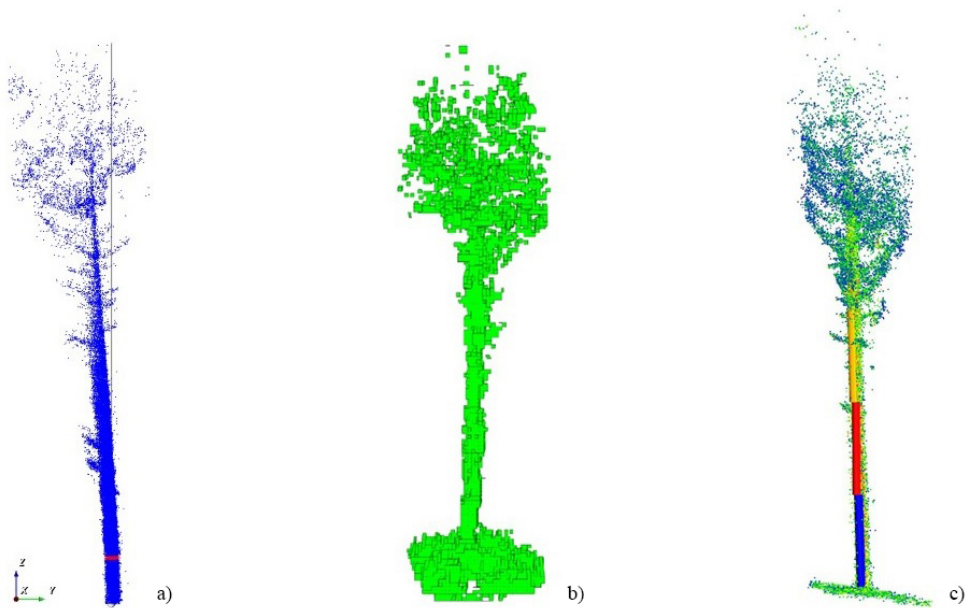


Figure 5: DBH extraction phases: a) DBH and Tree Height data extracted by 3D Forest; b) Voxelization by "VoxR" package; c) Reconstruction of the geometrical primitives with RANSAC on the points classified as stem.

292 compromising the correct data analysis. An interpolation of the two diameter
 293 values closest to the breast height (1.30 m) allowed to calculate each stem
 294 DBH. Furthermore, in this set, the barycentric coordinates of each point
 295 cloud tree and the DBH were extracted. Again, using the inventory data, we
 296 achieved the volumes of the cylinders, estimating them up to a height of 8 m
 297 above the ground. The maximum height was then extracted using the lidR
 298 package (Roussel et al., 2020). Finally, the "rLiDAR" package (Silva et al.,
 299 2018) was used for the calculation of the CBH. This package enables to find
 300 a set number classes of point clustered along the z-axis tree by "kmeans"
 301 algorithm. Thereby, for each subset was computed "Convex Hull" algorithm

302 which had facilitated the distinction of the crown from the trunk (Figure 6).



Figure 6: CBH estimated by Convex Hull function.

303 2.5. Comparison analysis

304 We evaluated the bias and root-mean-square error (RMSE) of selected
305 variables (DBH, H) comparing first the results gained with the three dif-
306 ferent algorithms ("3D Forest", "VoxR" and the combination of "TreeLS-
307 lidar-rLiDAR" packages) with ground-truth measures on felled trees; then,
308 comparing traditional field surveys and the best MLS method with ground
309 truth (adding CBH). We used the following equations:

$$bias = \sum_{i=1}^N \frac{x_i - x_{i,ref}}{N} \quad (2)$$

$$RMSE = \sqrt{\sum_{i=1}^N \frac{(x_i - x_{i,ref})^2}{N}} \quad (3)$$

310 where N is the number of felled trees, x_i refers to the estimates achieved
 311 with the algorithms and with traditional survey, and $x_{i,ref}$ refers to the corre-
 312 sponding ground truth value. Additionally, we used the following definitions
 313 for the relative bias and RMSE:

$$bias\% = \frac{bias}{x_{ref}} \times 100\% \quad (4)$$

314

$$RMSE\% = \frac{RMSE}{x_{ref}} \times 100\% \quad (5)$$

315 where x_{ref} is the mean of the reference values. For the comparison among the
 316 three MLS methods with ground truth measurement, we also evaluated the
 317 bias and RMSE for stem volume extraction up to 8 meters above the ground.
 318 We fitted regression lines of DBH and H values distribution derived by laser
 319 survey, traditional field operation and ground truth assessment data. Finally,
 320 we plotted all parameters distribution using boxplot charts and tested the
 321 differences of means using paired two-sided *t-test* with 95% of confidence
 322 level ($\alpha=0.05$).

323 **3. Results**

324 *3.1. Comparison of the three MLS methods for feature extraction*

325 Exploiting the object 3D reconstruction, we obtained the score with most
 326 accuracy, with the identification of the closest geometric primitive of its origi-
 327 nal shape. With this first analysis we wanted to discard the less accurate

328 method for a better comparison in the following step. The best accuracy
329 is reached with the "TreeLs-lidR-rLiDAR" packages combination (Table 2),
330 through the Hough transformation. We then performed a stem modelling
331 with the RANSAC algorithm, which allowed the more accurate estimation.
332 The use of MLS has produced zones with low density and high noise point
333 clouds (Figure 7).

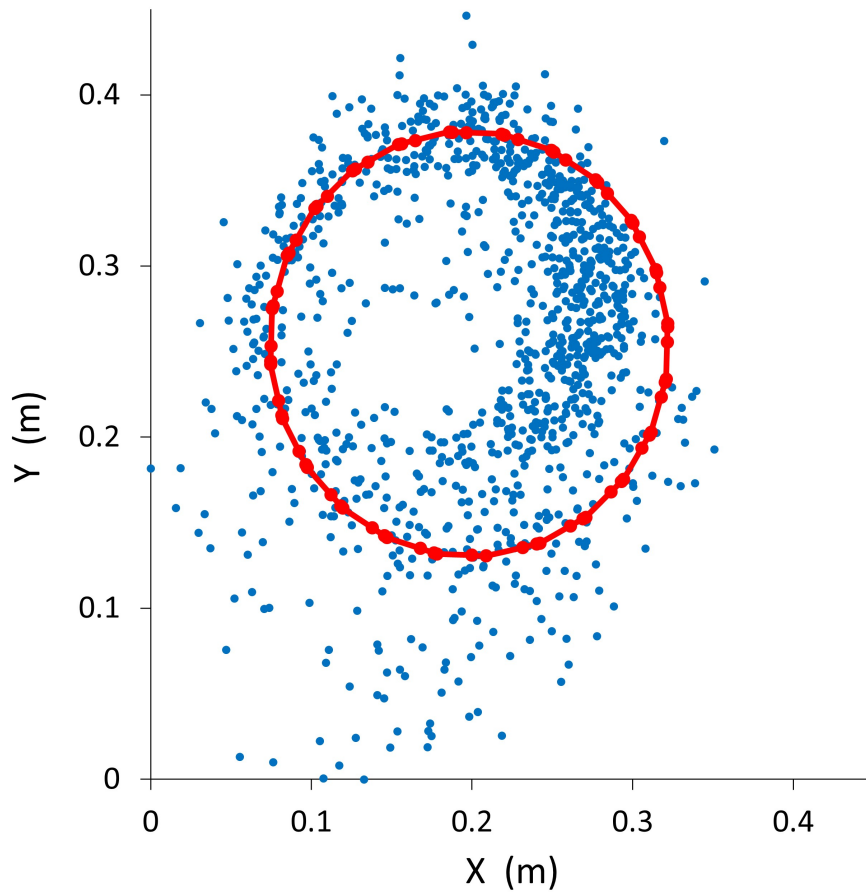


Figure 7: DBH points extracted and plotted on a 2D graph. Red dots are the ones used to interpolate with a suitable circle, while blue dots are the discarded ones.

Table 2: Comparison of DBH (diameter at breast height), H (tree height) and VOL (branch-free stem volume up to 8 meters) measures collected from the 50 felled trees and parameters estimated by different algorithms. In brackets standard deviation is reported for felled trees measures and percentage values for bias and RMSE.

	DBH (σ) [cm]		H (σ) [m]		VOL (σ) [m^3]	
FELLED	24.7 (5.2)		17.1 (1.2)		11.2 (1.5)	
Platform	Bias (%)	RMSE (%)	Bias (%)	RMSE (%)	Bias (%)	RMSE (%)
3D Forest	0.9 (3.8)	4.1 (16.3)	-2.4 (-14.4)	3.1 (18.3)	0.0 (-11.5)	0.1 (31.7)
VoxR	2.6 (10.4)	6.8 (27.0)	-1.7 (-9.9)	2.4 (14.0)	0.0 (-11.1)	0.1 (39.6)
TreeLS-lidr-rLiDAR	0.0 (0.0)	2.7 (10.8)	-1.5 (-8.6)	2.4 (13.9)	0.0 (-4.1)	0.0 (12.4)

334 *3.2. Comparison of traditional and MLS methods with ground truth*

335 Bias and RMSE values of traditional field sampling compared to ground
336 truth measurements are very low for DBH: 0.8% (0.2 cm) and < 5% (1.1 cm)
337 respectively (see Table 3). Similar gaps occur in tree sub-samples with DBH
338 below and above 25 cm (RMSE of 0.8 cm and 1.3 cm respectively). Manual
339 measured tree height was slightly underestimated compared to the ground
340 truth (% bias = -0.7 and % RMSE = 10.2) as well as in trees sub-sample
341 with heights below 17.5 m (bias % = -1.3 and RMSE % = 11.2) (Table 3).
342 Diversely, the RMSE of H estimates of trees higher than 17.5 m indicated a
343 minor overestimation (1.6 m and 8.9%) compared to the ground truth. CBH
344 showed a bias of 0.1 m (0.6%) and a higher RMSE (15.8%) (Table 3).

345 Comparing MLS values with ground truth measurements (Table 4), the
346 bias of DBH estimates was equal to 0 for both absolute and percent values
347 and the RMSE 10.8% (2.7 cm). For DBH sub-groups, we found opposite
348 estimates: positive for DBH below 25 cm (0.8 cm and 4.1%) and negative for
349 DBH above 25 cm (-0.8 cm and -2.8%); % RMSE was equal for both classes

Table 3: Tree variables values reached with traditional manual measurements on standing trees (TRAD) and from cut down trees (FELLED). Abs : absolute values; % : percent values.

Variable	N	Mean (σ)		Bias		RMSE	
		TRAD	FELLED	Abs	%	Abs	%
DBH [cm]	50	24.9 (5.4)	24.7 (5.2)	0.2	0.8	1.1	4.5
H [m]	50	17.0 (2.1)	17.1 (1.2)	-0.1	-0.7	1.7	10.2
CBH [m]	50	11.2 (1.4)	11.2 (1.5)	0.1	0.6	1.8	15.8
DBH \leq 25 [cm]	25	20.7 (3.4)	20.6 (3.4)	0.1	0.4	0.8	4.1
DBH $>$ 25 [cm]	25	29.2 (3.4)	28.9 (3.1)	0.3	1.1	1.3	4.6
H \leq 17.5 [m]	28	16.1 (2.0)	16.3 (1.0)	-0.2	-1.3	1.8	11.2
H $>$ 17.5 [m]	22	18.1 (1.8)	18.1 (0.5)	0.0	0.0	1.6	8.9
CBH \leq 17.5 [m]	28	11.2 (1.4)	11.1 (1.9)	0.1	0.7	1.9	17.5
CBH $>$ 17.5 [m]	22	11.2 (1.3)	11.2 (1.0)	0.05	0.5	1.5	13.2

350 (10.6%). H and CBH measured with MLS were underestimated compared to
351 the ground truth (bias of -8.6% for H and -13.3% for CBH) but CBH estimate
352 had the highest percent RMSE value (19.5%). Splitting the analysis by H
353 classes (below and above 17.5 m), both SLAM measures confirmed an overall
354 underestimation compared to the ground truth (bias % of -7.6 for H below
355 17.5 m and -9.8 for H above 17.5 m). **Branch-free** stem volume (up to 8
356 meters) values showed a bias and a RMSE of -4.1% (-0.01 m^3) and 12.4%
357 (0.04 m^3) respectively.

358 Figure 8a shows the overestimation of smaller DBH values and the un-
359 derestimation of greater values (red line) using MLS. The comparison of tree

Table 4: Tree parameters values measured with SLAM (MLS) and on the ground (FELLED). Abs : absolute values; % : percent values.

Variable	N	Mean (σ)		Bias		RMSE	
		MLS	FELLED	Abs	%	Abs	%
DBH [cm]	50	24.7 (5.1)	24.7 (5.2)	0.01	0.04	2.7	10.8
H [m]	50	15.6 (1.7)	17.1 (1.2)	-1.48	-8.64	2.4	13.9
CBH [m]	50	9.7 (1.1)	11.2 (1.5)	-1.48	-13.3	2.2	19.5
VOL [m^3]	50	0.31 (0.1)	0.32 (0.1)	-0.01	-4.1	0.04	12.4
DBH \leq 25 [cm]	25	21.4 (3.3)	20.6 (3.4)	0.8	4.1	2.2	10.6
DBH $>$25 [cm]	25	28.0 (4.3)	28.9 (3.1)	-0.8	-2.8	3.1	10.6
H \leq17.5 [m]	28	15.1 (1.7)	16.3 (1.0)	-1.2	-7.6	2.4	14.7
H $>$17.5 [m]	22	16.3 (1.6)	18.1 (0.5)	-1.8	-9.8	2.3	12.9
CBH \leq17.5 [m]	28	9.4 (1.2)	11.1 (1.9)	-1.7	-15.5	2.5	22.4
CBH $>$17.5 [m]	22	10.0 (1.0)	11.2 (1.0)	-1.2	-10.4	1.7	14.9

360 height (Figure 8b) reveals the same pattern of underestimation of MLS data
361 for the heighest trees. We did not detect statistical differences in mean DBH
362 ($\alpha=0.05$) between the two estimation methods (MLS and TRAD) compared
363 to the direct measurement on felled trees (Figure 9a), but we found them in
364 mean H (MLS vs FELLED) both for the whole sample (15.6 m vs 17.1 m re-
365 spectively) and splitting it by H classes (15.1 m vs 16.3 m for H<17.5 m and
366 16.3 m vs 18.1 m for H >17.5 m) (Figure 9b). We also detected significant
367 statistical differences in comparison of mean CBH (9.7 m for MLS vs 11.2 m
368 for felled trees) and for stem volume (0.31 m^3 for MLS vs 0.32 m^3 for felled
369 trees) (Figure 10).

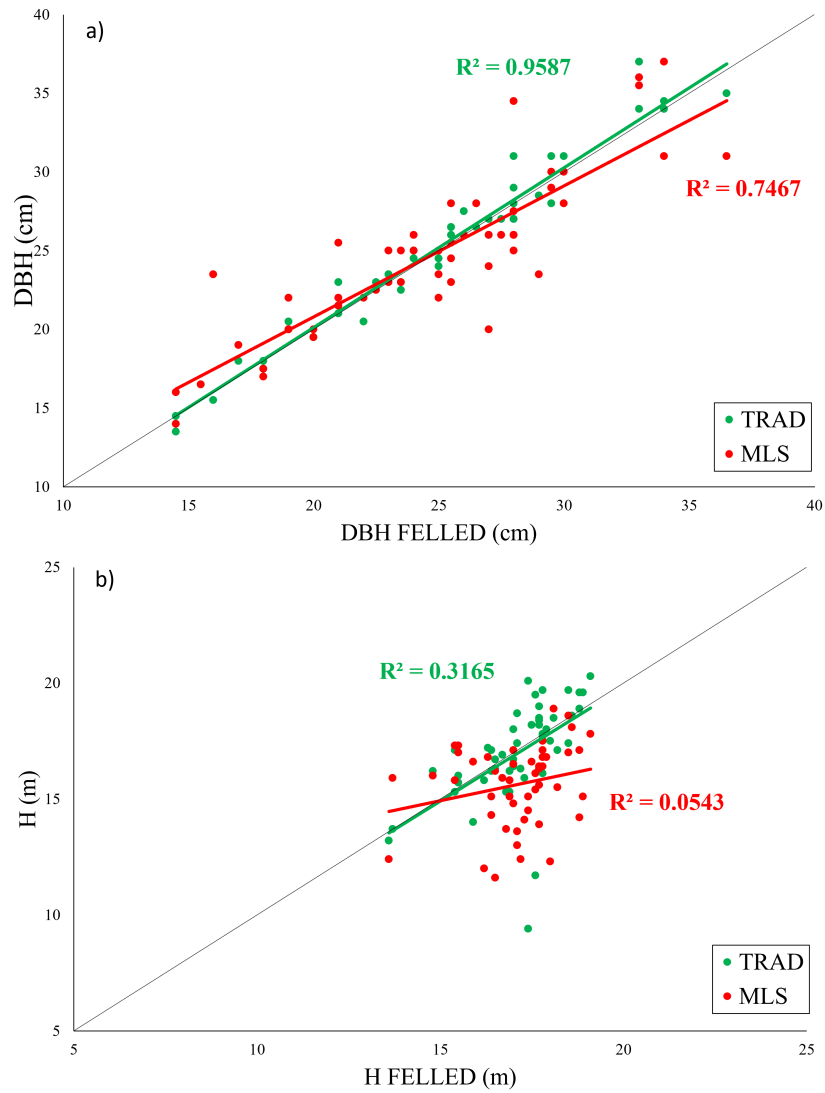


Figure 8: Regression analysis between DBH (a) and H (b) values derived by laser survey (MLS, red dots), traditional field operation (TRAD, green dots) and ground truth assessment data (FELLED).

370 4. Discussion

371 Forest structure and yield measurements are essential not only for com-
 372 puting timber productivity but also for calibrating any kind of multi-functional

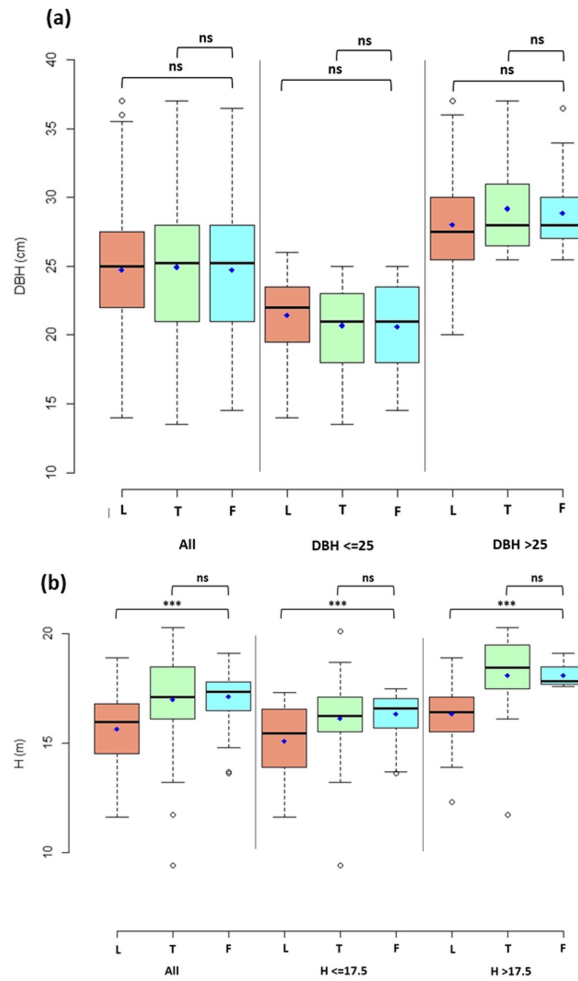


Figure 9: Boxplots of the DBH distribution (a) and tree height H (b) from MLS (L - red), TRADitional (T - green) and FELLEd trees measurement (F - blue) for the whole sample (All) and sub-samples (DBH below/above 25 cm and H below/above 17.5 m). Horizontal bold lines are medians, blue dots are the means. Whiskers are minimum and maximum values and circles are outliers. Significance of differences in DBH and H between MLS, TRAD and FELLEd are marked by "ns" (not significant, p-value > 0.1) or "***" (p-value < 0.001) tested with paired two-sided Student's t-Test.

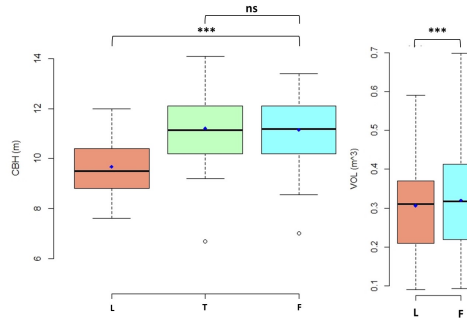


Figure 10: Boxplots showing the CBH distribution (a) the volume distribution (b) of the tree stems from SLAM laser technology (L - red), traditional (T - green) and field direct measurement of felled trees (F - blue), across the whole sample ($n = 50$). Horizontal bold lines are medians, blue dots are means. Whiskers are minimum and maximum values and circles are outliers. * = p value < 0.05 , ** = p value < 0.01 , *** = p value < 0.001 ; ns, not significant (paired and “two-sided” Student’s t-Test for laser and traditional measures with the ground truth).

373 forest management (e.g. biodiversity conservation, carbon sequestration and
 374 other ecosystem services). Nonetheless, accurate forestry measurements are
 375 not straightforward due to forests complexity and to the characteristics of
 376 the traditional instruments used in forest field measurements (e.g., calipers
 377 and clinometers). They are easy to use but they require several operational
 378 steps, becoming time consuming, laborious and expensive when repeated
 379 in inventory survey (Shao et al., 2020). MLS can provide very fast data
 380 collection of large areas, reducing the efforts for surface area and the mea-
 381 surement error. Holopainen et al. (2013b) compared the accuracy and the
 382 efficiency of TLS, ALS and MLS systems on 438 trees in an urban forest
 383 area in Finland. The study proves that TLS and MLS outperform ALS for
 384 the parameters detection, as the canopy effect hampers the achievement of

385 trustful results. Vatandaşlar and Zeybek (2021) evaluated the efficiency and
386 reliable of Zeb-Revo lidar (HMLS) by GeoSlam company compared to man-
387 ual field measurements, considered as ground truth, in a forest stand (79
388 ha) in Turkey. They reported that DBH RMSE was 2.41% and bias 0.56%,
389 while the timber volume showed a high deviation (21,5%), compared with al-
390 lometric values. Bauwens et al. (2016) compared TLS with a handheld MLS.
391 These two different systems, compared with the traditional field DBH mea-
392 surements, provided similar results with a bias < -0.2 cm and a RSME < 1.5
393 cm. The DBH detection was determined with an accuracy of < 3 cm scoring
394 96% for the TLS and 98% for the MLS. These rates decreased, respectively,
395 to 78% and 73% with < 1 cm accuracy. This confirms that TLS e MLS
396 produce comparable results in terms of accuracy, while the latter may result
397 convenient as it reduces the time spent for performing the survey and the
398 post processing phase of point cloud registration. Our results showed that
399 data collected with MLS survey in an dense even-aged black pine plantation,
400 provides acceptable DBH estimations, featuring a 10.8% RMSE respect to
401 ground truth (4.5% RMSE with traditional measurements). The accuracy
402 of DBH estimation with MLS remains sufficiently high at all size classes.
403 The error slightly increases with height measurements, ranging from 13.9%
404 for H and 19.5% for CBH, where traditional hypsometer survey produced
405 10.2% and 15.8% respectively. It is worth to note that our study confirms
406 the most recent findings in the literature; the accuracy of H estimations de-
407 creases when the tree height increases, highlighting some limitation of the
408 proposed approach. Consistently, the RMSE increases from the ground to
409 the top of the tree for two reasons: i) the crown, being more dense, generally

410 occlude the light beam by LiDAR; ii) the distance from the scanner to the
411 stem decreases both measurement accuracy and points resolution. Both of
412 these effects result in a smaller number of good quality arcs (Hyypä et al.,
413 2020b). The values achieved in this work are not very different from those
414 recorded in a Finland Boreal forest (Hyypä et al., 2020b) where the RMSE
415 for total tree height estimation, using a backpack mobile laser scanner, was
416 8.7%. From the statistical analysis, the authors reported a RMSE of stem
417 Volume computed in two sample plots, ranging from 0.053 m³ e 0.002m³.
418 The tree density in Boreal forests is usually much lower than in scarcely
419 thinned mountain conifer plantations where the standing trees treetops are
420 often hardly detectable. Considering our case with similar characteristics,
421 the RMSE value compared with felled trees is 0.004m³. A detection accu-
422 racy of 90.9% was reached for the DBH detection from a MLS based point
423 cloud compared with traditional ground data (Chen et al., 2019). This is
424 confirmed even in the article by Cabo et al. (2018), where TLS e ZEB REVO
425 are compared in *Pinus pinea* and *Platanus hispanica* plantations. In those
426 sites, DBH RMSE is 0.011 m e 0.009 m respectively and H RMSE of 1.340 m
427 and 9.440 m. Our approach produces comparable results with those already
428 described in the reviewed literature, despite the authors tested the methodol-
429 ogy with trees higher than 15 meters and in sunny conditions that reduce the
430 MLS accuracy. Kaarta Stencil 2 proved to be versatile and featuring higher
431 mobility if compared with TLS. The data processing method proposed in our
432 study provides the most robust denoising method was the Hough transforma-
433 tion, since it maintains stem features up to the tree crown, allowing a better
434 accuracy on the stem modelling phase. It worked out in good combination

435 with the cylinder fit Ransac algorithm for stem modelling. The proposed
436 workflow is linear and replicable to further studies as well the sample used.
437 Dealing with the CBH, the proposed method (Convex Hull) provides a 3D
438 graph showing the differences between the crown and the remaining stem,
439 enabling the CBH visualization. A more efficient approach could be the com-
440 bination of airborne collected data, for a more realistic detection of the crown
441 shape from the forest canopy top (Luo et al., 2018). Finally, an important
442 aspect that needs further studies is the effect of diameter size (Ryding et al.,
443 2020). In our study we have limited the detection to the dominant and regu-
444 larly shaped species, the black pine, providing more homogeneous target and
445 facilitating the data processing. The results obtained are encouraging but
446 need to be validated in more heterogeneous structures with mixed species
447 and multi-layer stands.

448 5. Conclusions

449 This study demonstrates the applicability of the hand held MLS with
450 SLAM algorithm for the estimation of metric parameters of individual trees
451 in a black pine (*Pinus nigra Arn.* plantation). The advantages of the MLS-
452 SLAM application transcend the automatic registration of the scans and the
453 low weight of the device, which favoured a high rate of reliability in retriev-
454 ing the 3D structure and forest monitoring. Statistical analysis between
455 LiDAR and ground truth data shows an accuracy of about 10% of relative
456 RMSE. The forest environment investigated had very dense and overlap-
457 ping crowns, and the presence of a consistent number of branches from 8
458 m height hindered the laser beam in acquiring objects at this height; this

459 limitation reduces the estimate of the maximum tree height and total stem
460 volume calculation. Our method exploited a semi-automatic procedure for
461 the branch-free stem volume estimation, even if few thresholding operations
462 are needed in the loop. Our research paves the way for future experiments,
463 by highlighting limitations that deserve further investigation. Firstly, the
464 sample stand is homogeneous both in terms of tree species and morphology;
465 the same approach should be tested in a more complex contexts. Secondly,
466 the lack of literature benchmarks in the definition of CBH. Indeed, the com-
467 parison with ground truth data is left to the operator’s subjectivity; a more
468 objective method of CBH extraction should be proposed in future research.
469 Finally, the estimation of H cannot be sufficiently accurate, and integration
470 with aerial data is still mandatory to guarantee a complete mapping of the
471 surveyed area. Nonetheless, remote sensing data will provide new and accu-
472 rate field data to improve measuring and estimation forest parameters, such
473 as basal area or stand volume.

474 **Acknowledgements**

475 We wish to thank the following people and institution: Fabio Piccinini
476 and Francesco Di Stefano for laser scanning support; Cristina Lucesole, Glo-
477 ria Nespola and Vittoria Bocchini for their help in field sampling; Dr. Nadia
478 Sabatini of the “Unione Montana Alta Valle del Metauro” for providing au-
479 thorization and logistic support (tree felling included).

480 **Funding**

481 This research did not receive any specific grant from funding agencies in
482 the public, commercial, or not-for-profit sectors.

483 **CRedit authorship contribution statement**

484 Stefano Chiappini: Data curation, Investigation, Methodology, Software,
485 Writing - original draft. Roberto Pierdicca: Data curation, Formal analy-
486 sis, Methodology, Writing - review and editing. Francesco Malandra: Data
487 curation, Formal analysis, Investigation, Writing - review and editing. En-
488 rico Tonelli: Data curation, Formal analysis, Investigation, Writing - re-
489 view and editing. Eva Savina Malinverni: Writing - review and editing.
490 Carlo Urbinati: Conceptualization, Funding acquisition, Resources, Writing
491 - review and editing. Alessandro Vitali: Conceptualization, Investigation,
492 Methodology, Supervision, Writing - review and editing.

493 **Declaration of Competing Interest**

494 The authors declare that they have no known competing financial inter-
495 ests or personal relationships that could have appeared to influence the work
496 reported in this paper.

497 **References**

498 Bauwens, S., Bartholomeus, H., Calders, K., Lejeune, P., 2016. Forest inven-
499 tory with terrestrial lidar: A comparison of static and hand-held mobile
500 laser scanning. *Forests* 7, 127. doi:<https://doi.org/10.3390/f7060127>.

- 501 Brede, B., Calders, K., Lau, A., Raunonen, P., Bartholomeus, H.M., Herold,
502 M., Kooistra, L., 2019. Non-destructive tree volume estimation through
503 quantitative structure modelling: Comparing uav laser scanning with ter-
504 restrial lidar. *Remote Sensing of Environment* 233, 111355.
- 505 Cabo, C., Del Pozo, S., Rodríguez-Gonzálvez, P., Ordóñez, C., Gonzalez-
506 Aguilera, D., 2018. Comparing terrestrial laser scanning (tls) and wearable
507 laser scanning (wls) for individual tree modeling at plot level. *Remote*
508 *Sensing* 10, 540.
- 509 Čerňava, J., Tuček, J., Koreň, M., Mokroš, M., 2017. Estimation of diameter
510 at breast height from mobile laser scanning data collected under a heavy
511 forest canopy. *Journal of Forest Science* 63, 433–441. doi:[https://doi.](https://doi.org/10.17221/28/2017-JFS)
512 [org/10.17221/28/2017-JFS](https://doi.org/10.17221/28/2017-JFS).
- 513 Chen, S., Liu, H., Feng, Z., Shen, C., Chen, P., 2019. Applicability of personal
514 laser scanning in forestry inventory. *PLoS One* 14, e0211392.
- 515 Chernov, N., Lesort, C., 2005. Least squares fitting of circles. *Journal of*
516 *Mathematical Imaging and Vision* 23, 239–252. doi:[https://doi.org/](https://doi.org/10.1007/s10851-005-0482-8)
517 [10.1007/s10851-005-0482-8](https://doi.org/10.1007/s10851-005-0482-8).
- 518 de Conto, T., Olofsson, K., Görgens, E.B., Rodriguez, L.C.E., Almeida, G.,
519 2017. Performance of stem denoising and stem modelling algorithms on
520 single tree point clouds from terrestrial laser scanning. *Computers and*
521 *Electronics in Agriculture* 143, 165–176. doi:[https://doi.org/10.1016/](https://doi.org/10.1016/j.compag.2017.10.019)
522 [j.compag.2017.10.019](https://doi.org/10.1016/j.compag.2017.10.019).

- 523 Dalla Corte, A.P., Rex, F.E., Almeida, D.R.A.d., Sanquetta, C.R., Silva,
524 C.A., Moura, M.M., Wilkinson, B., Zambrano, A.M.A., Cunha Neto,
525 E.M.d., Veras, H.F., et al., 2020. Measuring individual tree diameter
526 and height using gatoreye high-density uav-lidar in an integrated crop-
527 livestock-forest system. *Remote Sensing* 12, 863. doi:[https://doi.org/
528 10.3390/rs12050863](https://doi.org/10.3390/rs12050863).
- 529 Dassot, M., Colin, A., Santenoise, P., Fournier, M., Constant, T., 2012.
530 Terrestrial laser scanning for measuring the solid wood volume, including
531 branches, of adult standing trees in the forest environment. *Computers
532 and Electronics in Agriculture* 89, 86–93.
- 533 Del Perugia, B., Giannetti, F., Chirici, G., Travaglini, D., 2019. Influence
534 of scan density on the estimation of single-tree attributes by hand-held
535 mobile laser scanning. *Forests* 10, 277. doi:[https://doi.org/10.3390/
536 f10030277](https://doi.org/10.3390/f10030277).
- 537 Fernández-Sarría, A., Martínez, L., Velázquez-Martí, B., Sajdak, M., Es-
538 tornell, J., Recio, J., 2013. Different methodologies for calculating crown
539 volumes of *platanus hispanica* trees using terrestrial laser scanner and a
540 comparison with classical dendrometric measurements. *Computers and
541 Electronics in Agriculture* 90, 176–185. doi:[https://doi.org/10.1016/
542 j.compag.2012.09.017](https://doi.org/10.1016/j.compag.2012.09.017).
- 543 Forsman, M., Holmgren, J., Olofsson, K., 2016. Tree stem diameter estima-
544 tion from mobile laser scanning using line-wise intensity-based clustering.
545 *Forests* 7, 206. doi:<https://doi.org/10.3390/f7090206>.

- 546 Girardeau-Montaut, D., 2021. D.c. 3d p.c. and m.p.s.o.s.p. 2016. <https://www.danielgm.net/index.ph>. Accessed: 9 M. 2019.
- 547
- 548 Gollob, C., Ritter, T., Nothdurft, A., 2020. Forest inventory with long range
549 and high-speed personal laser scanning (pls) and simultaneous localization
550 and mapping (slam) technology. *Remote Sensing* 12, 1509.
- 551 Gollob, C., Ritter, T., Wassermann, C., Nothdurft, A., 2019. Influence of
552 scanner position and plot size on the accuracy of tree detection and diam-
553 eter estimation using terrestrial laser scanning on forest inventory plots.
554 *Remote Sensing* 11, 1602.
- 555 Hackel, T., Wegner, J.D., Schindler, K., 2016. Contour detection in unstruc-
556 tured 3d point clouds, in: *Proceedings of the IEEE conference on computer
557 vision and pattern recognition*, pp. 1610–1618.
- 558 Holmgren, J., Tulldahl, M., Nordlöf, J., Willén, E., Olsson, H., 2019. Mobile
559 laser scanning for estimating tree stem diameter using segmentation and
560 tree spine calibration. *Remote Sensing* 11, 2781. doi:[https://doi.org/
561 10.3390/rs11232781](https://doi.org/10.3390/rs11232781).
- 562 Holopainen, M., Kankare, V., Vastaranta, M., Liang, X., Lin, Y., Vaaja, M.,
563 Yu, X., Hyyppä, J., Hyyppä, H., Kaartinen, H., Kukko, A., Tanhuanpää,
564 T., Alho, P., 2013a. Tree mapping using airborne, terrestrial and mobile
565 laser scanning - a case study in a heterogeneous urban forest. *Urban
566 Forestry & Urban Greening* 12, 546–553. doi:[https://doi.org/10.1016/
567 j.ufug.2013.06.002](https://doi.org/10.1016/j.ufug.2013.06.002).

568 Holopainen, M., Kankare, V., Vastaranta, M., Liang, X., Lin, Y., Vaaja,
569 M., Yu, X., Hyyppä, J., Hyyppä, H., Kaartinen, H., et al., 2013b. Tree
570 mapping using airborne, terrestrial and mobile laser scanning—a case study
571 in a heterogeneous urban forest. *Urban forestry & urban greening* 12, 546–
572 553.

573 Hyyppä, E., Hyyppä, J., Hakala, T., Kukko, A., Wulder, M.A., White, J.C.,
574 Pyörälä, J., Yu, X., Wang, Y., Virtanen, J.P., et al., 2020a. Under-canopy
575 uav laser scanning for accurate forest field measurements. *ISPRS Journal*
576 *of Photogrammetry and Remote Sensing* 164, 41–60.

577 Hyyppä, E., Kukko, A., Kaijaluoto, R., White, J.C., Wulder, M.A., Pyörälä,
578 J., Liang, X., Yu, X., Wang, Y., Kaartinen, H., et al., 2020b. Accurate
579 derivation of stem curve and volume using backpack mobile laser scanning.
580 *ISPRS Journal of Photogrammetry and Remote Sensing* 161, 246–262.

581 Iizuka, K., Hayakawa, Y.S., Ogura, T., Nakata, Y., Kosugi, Y., Yonehara, T.,
582 2020. Integration of multi-sensor data to estimate plot-level stem volume
583 using machine learning algorithms—case study of evergreen conifer planted
584 forests in japan. *Remote Sensing* 12, 1649.

585 Itakura, K., Hosoi, F., 2020. Automatic tree detection from three-
586 dimensional images reconstructed from 360 spherical camera using yolo v2.
587 *Remote Sensing* 12, 988. doi:<https://doi.org/10.3390/rs12060988>.

588 Karna, Y.K., Penman, T.D., Aponte, C., Bennett, L.T., 2019. Assessing
589 legacy effects of wildfires on the crown structure of fire-tolerant eucalypt

590 trees using airborne lidar data. *Remote Sensing* 11, 2433. doi:<https://doi.org/10.3390/rs11202433>.
591

592 Kruček, M., Král, K., Cushman, K., Missarov, A., Kellner, J.R., 2020.
593 Supervised segmentation of ultra-high-density drone lidar for large-area
594 mapping of individual trees. *Remote Sensing* 12, 3260. doi:<https://doi.org/10.3390/rs12193260>.
595

596 Kukko, A., Kaartinen, H., Hyypä, J., Chen, Y., 2012. Multiplatform mobile
597 laser scanning: Usability and performance. *Sensors* 12, 11712–11733.

598 Kunz, M., Fichtner, A., Härdtle, W., Raunonen, P., Bruelheide, H., von
599 Oheimb, G., 2019. Neighbour species richness and local structural vari-
600 ability modulate aboveground allocation patterns and crown morphology
601 of individual trees. *Ecology Letters* 22, 2130–2140.

602 Lau, A., Bentley, L.P., Martius, C., Shenkin, A., Bartholomeus, H., Rau-
603 monen, P., Malhi, Y., Jackson, T., Herold, M., 2018. Quantifying branch
604 architecture of tropical trees using terrestrial lidar and 3d modelling. *Trees*
605 32, 1219–1231.

606 Lecigne, B., Delagrangé, S., Messier, C., 2018. Exploring trees in three
607 dimensions: Voxr, a novel voxel-based r package dedicated to analysing
608 the complex arrangement of tree crowns. *Annals of botany* 121, 589–601.
609 doi:<https://doi.org/10.1093/aob/mcx095>.

610 Liu, C., Xing, Y., Duanmu, J., Tian, X., 2018a. Evaluating different methods
611 for estimating diameter at breast height from terrestrial laser scanning.
612 *Remote Sensing* 10, 513. doi:<https://doi.org/10.3390/rs10040513>.

- 613 Liu, G., Wang, J., Dong, P., Chen, Y., Liu, Z., 2018b. Estimating individ-
614 ual tree height and diameter at breast height (dbh) from terrestrial laser
615 scanning (tls) data at plot level. *Forests* 9, 398.
- 616 Luo, H., Wang, L., Wu, C., Zhang, L., 2018. An improved method for im-
617 pervious surface mapping incorporating lidar data and high-resolution im-
618 agery at different acquisition times. *Remote Sensing* 10, 1349. doi:<https://doi.org/10.3390/rs10091349>.
- 620 Luoma, V., Saarinen, N., Wulder, M.A., White, J.C., Vastaranta, M.,
621 Holopainen, M., Hyyppä, J., 2017. Assessing precision in conventional
622 field measurements of individual tree attributes. *Forests* 8, 38. doi:<https://doi.org/10.3390/f8020038>.
- 624 Maguya, A.S., Tegel, K., Junttila, V., Kauranne, T., Korhonen, M., Burns,
625 J., Leppanen, V., Sanz, B., 2015. Moving voxel method for estimating
626 canopy base height from airborne laser scanner data. *Remote Sensing* 7,
627 8950–8972. doi:<https://doi.org/10.3390/rs70708950>.
- 628 Markku, Å., Raumonon, P., Kaasalainen, M., Casella, E., 2015. Analysis of
629 geometric primitives in quantitative structure models of tree stems. *Re-*
630 *mote Sensing* 7, 4581–4603.
- 631 Moe, K.T., Owari, T., Furuya, N., Hiroshima, T., 2020. Comparing indi-
632 vidual tree height information derived from field surveys, lidar and uav-
633 dap for high-value timber species in northern japan. *Forests* 11, 223.
634 doi:<https://doi.org/10.3390/f11020223>.

- 635 Mohan, M., Silva, C.A., Klauberg, C., Jat, P., Catts, G., Cardil, A., Hudak,
636 A.T., Dia, M., 2017. Individual tree detection from unmanned aerial ve-
637 hicle (uav) derived canopy height model in an open canopy mixed conifer
638 forest. *Forests* 8, 340. doi:<https://doi.org/10.3390/f8090340>.
- 639 Mokroš, M., Mikita, T., Singh, A., Tomašík, J., Chudá, J., Wežyk, P.,
640 Kuželka, K., Surovỳ, P., Klimánek, M., Zieba-Kulawik, K., et al., 2021.
641 Novel low-cost mobile mapping systems for forest inventories as terres-
642 trial laser scanning alternatives. *International Journal of Applied Earth
643 Observation and Geoinformation* 104, 102512.
- 644 Momo Takoudjou, S., Ploton, P., Sonké, B., Hackenberg, J., Griffon, S.,
645 De Coligny, F., Kamdem, N.G., Libalah, M., Mofack, G.I., Le Moguédec,
646 G., et al., 2018. Using terrestrial laser scanning data to estimate large
647 tropical trees biomass and calibrate allometric models: A comparison with
648 traditional destructive approach. *Methods in Ecology and Evolution* 9,
649 905–916.
- 650 Müller, A., Olschewski, R., Unterberger, C., Knoke, T., 2020. The valu-
651 ation of forest ecosystem services as a tool for management planning—a
652 choice experiment. *Journal of Environmental Management* 271, 111008.
653 doi:<https://doi.org/10.1016/j.jenvman.2020.111008>.
- 654 Nurunnabi, A., Sadahiro, Y., Lindenbergh, R., 2017. Robust cylinder fit-
655 ting in three-dimensional point cloud data. *International Archives of the
656 Photogrammetry, Remote Sensing and Spatial Information Sciences* 42.
- 657 Panagiotidis, D., Abdollahnejad, A., 2021a. Accuracy assessment of total

- 658 stem volume using close-range sensing: *Advances in precision forestry.*
659 *Forests* 12, 717.
- 660 Panagiotidis, D., Abdollahnejad, A., 2021b. Reliable estimates of mer-
661 chantable timber volume from terrestrial laser scanning. *Remote Sensing*
662 13. URL: <https://www.mdpi.com/2072-4292/13/18/3610>, doi:10.3390/
663 rs13183610.
- 664 Panagiotidis, D., Surovỳ, P., Kuželka, K., 2016. Accuracy of structure from
665 motion models in comparison with terrestrial laser scanner for the analysis
666 of dbh and height influence on error behaviour. *Journal of Forest Science*
667 62, 357–365.
- 668 Pierzchała, M., Giguère, P., Astrup, R., 2018. Mapping forests using an
669 unmanned ground vehicle with 3d lidar and graph-slam. *Computers and*
670 *Electronics in Agriculture* 145, 217–225. doi:[https://doi.org/10.1016/](https://doi.org/10.1016/j.compag.2017.12.034)
671 [j.compag.2017.12.034](https://doi.org/10.1016/j.compag.2017.12.034).
- 672 Puliti, S., Breidenbach, J., Astrup, R., 2020. Estimation of forest grow-
673 ing stock volume with uav laser scanning data: can it be done without
674 field data? *Remote Sensing* 12, 1245. doi:[https://doi.org/10.3390/](https://doi.org/10.3390/rs12081245)
675 [rs12081245](https://doi.org/10.3390/rs12081245).
- 676 R Core Team, 2021. R: A Language and Environment for Statistical Com-
677 puting. R Foundation for Statistical Computing. Vienna, Austria. URL:
678 <https://www.R-project.org/>.
- 679 Roussel, J.R., Auty, D., Coops, N.C., Tompalski, P., Goodbody, T.R.,
680 Meador, A.S., Bourdon, J.F., de Boissieu, F., Achim, A., 2020. lidar: An

681 r package for analysis of airborne laser scanning (als) data. *Remote Sensing of Environment* 251, 112061. URL: <https://www.sciencedirect.com/science/article/pii/S0034425720304314>, doi:<https://doi.org/10.1016/j.rse.2020.112061>.

682
683
684

685 Rusu, R.B., Cousins, S., 2011. 3d is here: Point cloud library (pcl), in: 2011
686 IEEE international conference on robotics and automation, IEEE. pp. 1–4.
687 doi:10.1109/ICRA.2011.5980567.

688 Ryding, J., Williams, E., Smith, M.J., Eichhorn, M.P., 2020. Assessing
689 handheld mobile laser scanners for forest surveys. *Remote Sensing* 7, 1095–
690 1111. doi:<https://doi.org/10.3390/rs70101095>.

691 Shao, J., Zhang, W., Mellado, N., Wang, N., Jin, S., Cai, S., Luo, L.,
692 Lejemble, T., Yan, G., 2020. Slam-aided forest plot mapping combining
693 terrestrial and mobile laser scanning. *ISPRS Journal of Photogrammetry and Remote Sensing* 110, 214–230. doi:<https://doi.org/10.1016/j.isprsjprs.2020.03.008>.

694
695

696 Sibona, E., Vitali, A., Meloni, F., Caffo, L., Dotta, A., Lingua, E., Motta, R.,
697 Garbarino, M., 2017. Direct measurement of tree height provides different
698 results on the assessment of lidar accuracy. *Forests* 8, 7. doi:<https://doi.org/10.3390/f8010007>.

699

700 Srinivasan, S., Popescu, S.C., Eriksson, M., Sheridan, R.D., Ku, N.W.,
701 2015. Terrestrial laser scanning as an effective tool to retrieve tree level
702 height, crown width, and stem diameter. *Remote Sensing* 7, 1877–1896.
703 doi:<https://doi.org/10.3390/rs70201877>.

704 Stovall, A.E., Vorster, A.G., Anderson, R.S., Evangelista, P.H., Shugart,
705 H.H., 2017. Non-destructive aboveground biomass estimation of coniferous
706 trees using terrestrial lidar. *Remote Sensing of Environment* 200, 31–42.

707 Gonzalez de Tanago, J., Lau, A., Bartholomeus, H., Herold, M., Avitabile,
708 V., Raumonon, P., Martius, C., Goodman, R.C., Disney, M., Manuri, S.,
709 et al., 2018. Estimation of above-ground biomass of large tropical trees
710 with terrestrial lidar. *Methods in Ecology and Evolution* 9, 223–234.

711 Tao, S., Wu, F., Guo, Q., Wang, Y., Li, W., Xue, B., Hu, X., Li, P.,
712 Tian, D., Li, C., et al., 2015. Segmenting tree crowns from terrestrial
713 and mobile lidar data by exploring ecological theories. *ISPRS Jour-*
714 *nal of Photogrammetry and Remote Sensing* 110, 66–76. doi:[https:](https://doi.org/10.1016/j.isprsjprs.2015.10.007)
715 [//doi.org/10.1016/j.isprsjprs.2015.10.007](https://doi.org/10.1016/j.isprsjprs.2015.10.007).

716 Team, R.C., et al., 2013. R: A language and environment for statistical
717 computing .

718 Tompalski, P., White, J.C., Coops, N.C., Wulder, M.A., 2019. Quantifying
719 the contribution of spectral metrics derived from digital aerial photogram-
720 metry to area-based models of forest inventory attributes. *Remote Sens-*
721 *ing of Environment* 234, 111434. doi:[https://doi.org/10.1016/j.rse.](https://doi.org/10.1016/j.rse.2019.111434)
722 [2019.111434](https://doi.org/10.1016/j.rse.2019.111434).

723 Trochta, J., Kruček, M., Vrška, T., Král, K., 2017. 3d forest: An application
724 for descriptions of three-dimensional forest structures using terrestrial li-
725 dar. *PLoS One* 12, e0176871. doi:[https://doi.org/10.1371/journal.](https://doi.org/10.1371/journal.pone.0176871)
726 [pone.0176871](https://doi.org/10.1371/journal.pone.0176871).

- 727 Van Brummelen, J., O'Brien, M., Gruyer, D., Najjaran, H., 2018. Au-
728 tonomous vehicle perception: The technology of today and tomorrow.
729 Transportation research part C: emerging technologies 89, 384–406.
- 730 Vatandaşlar, C., Zeybek, M., 2021. Extraction of forest inventory parameters
731 using handheld mobile laser scanning: A case study from trabzon, turkey.
732 Measurement 177, 109328.
- 733 Wang, Y., Lehtomäki, M., Liang, X., Pyörälä, J., Kukko, A., Jaakkola, A.,
734 Liu, J., Feng, Z., Chen, R., Hyypä, J., 2019. Is field-measured tree height
735 as reliable as believed—a comparison study of tree height estimates from
736 field measurement, airborne laser scanning and terrestrial laser scanning in
737 a boreal forest. ISPRS journal of photogrammetry and remote sensing 147,
738 132–145. doi:<https://doi.org/10.1016/j.isprsjprs.2018.11.008>.
- 739 Zaforemska, A., Xiao, W., Gaulton, R., 2019. Individual tree detection from
740 uav lidar data in a mixed species woodland. International Archives of the
741 Photogrammetry, Remote Sensing & Spatial Information Sciences .
- 742 Zhang, W., Wan, P., Wang, T., Cai, S., Chen, Y., Jin, X., Yan, G., 2019.
743 A novel approach for the detection of standing tree stems from plot-level
744 terrestrial laser scanning data. Remote sensing 11, 211. doi:<https://doi.org/10.3390/rs11020211>.
- 746 Zhou, S., Kang, F., Li, W., Kan, J., Zheng, Y., He, G., 2019. Extract-
747 ing diameter at breast height with a handheld mobile lidar system in an
748 outdoor environment. Sensors 19, 3212. doi:<https://doi.org/10.3390/s19143212>.
- 749

Declaration of interests

The authors declare that they have no known competing financial interests or personal relationships that could have appeared to influence the work reported in this paper.

The authors declare the following financial interests/personal relationships which may be considered as potential competing interests:

480 **Funding**

481 This research did not receive any specific grant from funding agencies in
482 the public, commercial, or not-for-profit sectors.

483 **CRedit authorship contribution statement**

484 Stefano Chiappini: Data curation, Investigation, Methodology, Software,
485 Writing - original draft. Roberto Pierdicca: Data curation, Formal analy-
486 sis, Methodology, Writing - review and editing. Francesco Malandra: Data
487 curation, Formal analysis, Investigation, Writing - review and editing. En-
488 rico Tonelli: Data curation, Formal analysis, Investigation, Writing - re-
489 view and editing. Eva Savina Malinverni: Writing - review and editing.
490 Carlo Urbinati: Conceptualization, Funding acquisition, Resources, Writing
491 - review and editing. Alessandro Vitali: Conceptualization, Investigation,
492 Methodology, Supervision, Writing - review and editing.

493 **Declaration of Competing Interest**

494 The authors declare that they have no known competing financial inter-
495 ests or personal relationships that could have appeared to influence the work
496 reported in this paper.

497 **References**

498 Bauwens, S., Bartholomeus, H., Calders, K., Lejeune, P., 2016. Forest inven-
499 tory with terrestrial lidar: A comparison of static and hand-held mobile
500 laser scanning. *Forests* 7, 127. doi:<https://doi.org/10.3390/f7060127>.